Stable Mechanical Fixation in a Bionic Osteochondral Scaffold Considering Bone Growth

Jian Zhou, Hao Huang, Lijing Wang, Maryam Tamaddon, Chaozong Liu, Tengbo Yu*， Ziyu Liu*, Yingze Zhang

Jian Zhou and Hao Huang have contributed equally to this work.
J. Zhou
Department of Orthopedic Surgery, Qingdao Municipal Hospital, Qingdao University, Qingdao 266071, China
Z.-Y. Liu*, M. Tamaddon, C.-Z. Liu
Division of Surgery & Interventional Science, University College London, Royal National Orthopaedic Hospital, Stanmore HA7 4LP, London, UK
e-mail:liu_ziyu@buaa.edu.cn
Z.-Y. Liu*, H.Huang,
School of Engineering Medicine, Beihang University, Beijing 100191, China
L.-J. Wang, Z.-Y. Liu*
School of Aeronautic Science and Engineering, Beihang University, Beijing 100191, China
J. Zhou, T.-B. Yu*, Y.-Z. Zhang
Department of Sports Medicine, Affiliated Hospital of Qingdao University, Qingdao 266000, China
e-mail:ytb8912@163.com

Abstract
In the field of tissue engineering, there is significant subsidence of the porous design scaffold several months after implantation. To avoid stress shielding, high scaffold porosity is often set, aiming to diminish mechanical properties of the scaffold. The more close the mechanical properties of the scaffold to surrounding tissues, the better bioperformance it will get. Besides, adequate mechanical stability is needed as the scaffold needs to be well fixed in the target area and it will endure load after surgery. Evaluating the mechanical fixation of the scaffold at the initial stage and the long-term performance of a scaffold for *in vivo* study is hard, as no facility can be put into the target area for the friction test. Finite element analysis is one of the optimal ways to solve this problem, and it can help researchers to investigate mechanical behaviors of implants. Further, it offers an alternative approach to evaluating the scaffold designs prior to conducting physical tests.

Keywords：Osteochondral scaffold; mechanical fixation; scaffold subsidence; finite element analysis

Statements and Declarations
The authors declare that the research was conducted in the absence of any commercial or financial relationships that could be construed as a potential conflict of interest.

Article Highlights:

- Mechanical stability of the biomimetic scaffold at the initial stage of implantation investigation
- Finite element models for scaffold with new regenerated bone tissue are developed based on *in vivo* tests
- Regenerated bone tissue in the scaffold quantification

1 Introduction

Tissue engineering, a multi-disciplinary technology, provides a porous biomaterial known as a scaffold as a medical application which could potentially increase the opportunity for tissue regeneration[1-3]. With the ultimate aim of high quality osteogenesis and cartilage regeneration, a scaffold's morphology, mechanical and biological function should mimic the properties of bone[4-6]. It is therefore crucial to understand the compositition and biomechanical properties of the bone before designing an osteochondral scaffold. The osteochondral unit consists of 3 main parts from top to bottom, which is cartilage, the subchondral bone plate, and the trabecular bone, which is composed of 10-20% of collagen, 9-20% of water, and 60-70% of bone mineral by weight[7]. The subcondral bone plate has a high Young's modulus similar to the cortical bone, providing mechanical support to load bearing. While the trabecular bone has a lower Young's modulus with special alignment to dampen the effect of sudden loading[8].

An osteocondral scaffold should be designed as close as possible to the osteochondral bone with regards to its geomagical, chemical, biomechanical, and biological properties. To mimic the geomagical properties of osteochondral bone, a three-dimensional multi-layer scaffold with the trabecular bone in the surrounding area should have a high porosity and inter-connected pore network[9]. In general, hydrogels such as polylactic acid (PLA) and poly (lactic-co-glycolic acid) (PLGA), etc., are used for cartilage regeneration[10-13]. These biomaterials can provide a three-dimensional template for mesenchymal stem cell (BMSCs) proliferation, migration and differentiation, and can also provide mechanical support which is similar to cartilage [6]. With regards to osteogenesis, titanium alloys are widely used due to their excellent biocompability, mechanical properties and chemical stability. High porosity scaffolds with reduced stiffness can avoid stress shielding, so as not to hinder bone remodeling and reabsorption[14, 15]. Highly interconnected pore nets with 100-400 μm pore size are considered optimal for bone regeneration [16-18].

The osteochondral scaffold should have adequate mechanical stability to enable initial fixation with the host tissues during implantation, as well as enduring loads after the surgery[19] . However, for clinical applications, the porous design results in diminished mechanical properties. If an implantation is partially or completely detached, it will fail *in vivo*, causing significant locking or catching at the target area of patients[20, 21].

The porosity and pore size are strongly related to the mechanical properties, and it is believed that high porosity with similar mechanical properties to the natural bone tissues would produce a positive clinical outcome[22] . As a permanent orthopaedic implant, the scaffold should not only have good mechanical fixation with the surrounding tissues, but also ensure safety over a long period of life after surgery. There is contradiction in scaffold design between the pore size, porosity and the strength as well as fatigue life.

Evaluating the mechanical fixation of the scaffold at the initial stage and the long-term performance of the scaffold *in vivo* is difficult and time consuming. Finite element analysis of the mechanical behaviors of implants offers an alternative approach to evaluating the scaffold design prior to physical tests.

This paper was aimed to investigate the mechanical stability of the biomimetic scaffold at the initial stage of implantation. According to previous in-vivo study (in sheep, n=5), scaffold could not maintain its original position and would sink 1-2 mm in the target area. To further explore the main reason, finite element models was developed and the physical model of scaffold with new regenerated bone tissue is created based by sheep femoral condyle image analysis. The FE model is to evaluate the subsidence main factor is compression or other related factors.

2 Material and methods

2.1 Ethical aspects and animals

Five young female sheep with a mean weight of 81.6 ± 6.4 kg were treated according to Animals (Scientific Procedures) Act (ASPA). Animal housing, feeding, examinations and care were conducted using established procedures.

2.2 Bionic scaffold osteogenesis quantification

In order to heal the cartilage defect, the novel osteochondral scaffold is designed to mimic osteochondral bone in compliance with structural, bio-mechanical and bio-functional properties which provide a suitable environment for osteogenesis and cartilage regeneration (Fig. 1) [23].

The top layer is made with PLGA infiltrated collagen with 8.5 mm diameter. The middle layer is made of medium polylactic acid PLA sterilized with 70% ethanol for 15 mins. The top structure of PLA is designed by layer junction, and each column bar is 0.5 mm in diameter and arranged in the same direction. The bottom layer is a 6 mm-tall truncated cone (8 mm diameter at the top and 5.9 mm diameter at the bottom) manufactured with a EOS M270 3D printer using pure titanium powder in the Direct Metal Laser Sintering (DMLS) method. The collagen layer was produced from monomeric collagens (pepsin and acid extracted). The collagen gels were then crosslinked to increase geometry stability. After that, they were impregnated with 10% PLGA solutions and dried using the Critical Point Drying method. To combine the titanium layer and the PLA layer, hot fusion is used whereby a partially melted PLA lattice is pressed into the Ti matrix, fusing the two layers together. To attach the collagen-PLGA layer to the rest of the scaffold, Ti-PLA is partially submerged into the crosslinked collagen suspension before freezing. After freeze-drying, a physical interlocking is achieved between the collagen-PLGA and Ti-PLA layers.

In terms of the bone structure, the osteochondral bone is constructed of three main parts from top to bottom, which are the cartilage, the subchondral bone plate, and the trabecular bone, the bionic scaffold is designed with 3 different materials. From bottom to top, the titanium layer was designed with 78.6% porosity and 1 mm * 1 mm square pore size to mimic the trabecular bone, which has a porosity of 50-90%, is composed of hydroxyapatite (Ca10 (PO4)6(OH)2), and has a pore size of around 1 mm in diameter [24]. Admittedly, an ideal structure for the osteogenesis and the substitute trabecular bone should achieve a spongy structure, but this kind of structure is hard to print and the main drawbacks are lacking of mechanical properties and a tendency to break. Therefore, to provide sufficient mechanical stimuli for bone regeneration, the titanium layer was designed as a truncated cone.

As for bio-mechanical properties, AX-10 Young's modulus (1-2Mpa) was designed to mimic cartilage Young's modulus which is around 0.95-1.69 Mpa [25]. As AX-10 doesn't have the same higher elasticity as cartilage, crosslink PLA junction layer was designed to provide enough mechanical support. The subchondral bone plate, an irregular thin plate located beneath the articular cartilage connected with the trabecular bone, has a high strength of 635±94 Mpa [26]. The PLA dense layer with 2200 Mpa strength was designed to mimic the bone plate mechanical properties. The bottom layer of the scaffold was made with pure titanium with 70-100 Mpa strength to substitute the trabecular bone (19±7 Mpa) [27].

Further, biofunctional properties should also be considered for scaffold design. Hazelton et al. mentioned that synovial fluid may cause low osteogenesis, which means that synovial fluid flow to the trabecular bone area should be prohibited [28, 29]. The PLA dense layer was deisgned for separating synovial fluid and bone marrow for cartilage and bone regeneration.

The pure titanium scaffold is manufactured with commercially EOS Titanium TiCP grade 2 powders which is created especially on EOSINT M system. The density of the powder is 4.5 g/cm^3.

According to the Animals (Scientific Procedures) Act (ASPA), all 5 young sheep with an average weight of 82kg were treated with sufficient food and water in a free land, and every examination and housing is based on established procedures. After the osteochondral defect was created and the scaffold was put into the hole, the sheep were housed individually for 5 days and treated with analgesia (Carprofen 5 mg/kg) and antibiotics (Enrofloxacin 10 mg/kg) subcutaneously twice a day.

After 3 months, the animals were euthanized and surrounding tissues with the scaffold were cut into several slices and scanned with a Niko XT H 225 machine. The reason for obtaining the regenerated bone tissues by analyzing 2D images rather 3D ones is that with 2D images it is easier to quantify tissue ingrowth. Slices from different areas are selected to analyze the tissue percentage in each scaffold hole and the percentage are averaged by 3 regions shown in Fig. 2. To obtain the percentage of bone regeneration in each pore of the scaffold, 2D Micro-CT scanned images were analyzed with MATLAB program.

2.3 Mechanical assessment model and simulation

As the scaffold structure is not axisymmetric but centro-symmetric, the scaffold is divided into 3 regions, which are edge, sub-mid and middle. The bone tissue percentage of each hole in that area is arithmetic mean of the real bone percentage value and each hole has the same bone tissue percentage at each area (Fig. 3). The regenerated bone percentages are shown below, which are used to generate a physical model for finite element.

2.4 Finite element models and boundary conditions

The main working condition in tissue engineering is friction. And one of the factors with the greatest influence on friction simulation is friction contact. In general, contact is defined as the touching of solid bodies at one or more points [30]. In this model, it aims to investigate deformation of scaffold and surrounding trabecular bone tissues in the presence of frictional forces.

The three physical models are designed with a 0% initial bone ingrowth, a 3-month bone ingrowth, and a 100% bone ingrowth respectively. In the 0% bone ingrowth model, the scaffold is set in frictional contact with surrounding bone tissues; in the model with 3 months' of bone ingrowth, the scaffold is set to bond with regenerated tissues and surrounding tissues, but in frictional contact with bottom surrounding tissue face; in that with 100% bone ingrowth, it is set to bond with regenerated tissues and all surrounding tissue faces. The contact is calculated in the Augmented Lagrange method.

Originally, the scaffold is designed as a truncated cone 8 mm in diameter for the top surface and 5.9 mm in diameter for the bottom surface. Each beam in the inner structure is 0.5 mm in diameter and each beam is 1.5 mm away from the neighbor beam from center to center.

Before the scaffold is placed into the defect, it is soaked in bone marrow concentrate to allow BMSCs to infiltrate into the scaffold. Then, the BMSCs infiltrated scaffold is implanted into the pre-created osteochondral defect (

Fig. **4**). After 3 months' post-surgery, new bone tissues have already regenerated in the scaffold. As tissues are distributed three-dimensionally, but mostly attached onto the scaffold beam surface, the physical model can be simplified by the regenerated bone ingrowth percentage of in-vivo tests. For instance, pore number 1-2 porosity is 39.4% found by the above chart, which means that 60.6% of the area is empty in a unit pore. As the bone percentage is analyzed by image and the sample is cut into slices, several new bone tissues may have been lost during the cutting process. In that case, as the bone percentage is lower than the actual bone percentage, it is assumed that the void space is a cubic structure occupied in a 1 mm^3 unit cubic pore of 60.6% (Fig. 5). The length of the void cubic structure is calculated by cubic root of 0.606 mm^3 which is 0.846 mm.

As the scaffold is put in the osteochondral defect, the trabecular bone hole in the bulk is seen as the same size as the scaffold titanium layer size. The lengths from the scaffold top surface edge to the trabecular bone's edge and from the scaffold bottom face to the bottom face of the trabecular bone are 4 mm. In this Finite Element (FE) model, the titanium alloy scaffold density is set as $4.5*10^3$ kg/m^3, the Young's modulus is set as 6500 Mpa, and the Poisson's ratio is 0.342. As for the trabecular bone whose density is set as 900 kg/m^3, the Young's modulus and the Poisson's ratio are set as 1600 Mpa and 0.12

respectively. In the model of 0% bone ingrowth (Fig. 6), as there is no bone ingrowth in the scaffold, the contact type between the scaffold and surrounding tissues (trabecular bone) is friction, and the friction coefficient is set as 0.42. Normal stiffness factor is 0.6, the amount of penetration between contact and target surfaces. In the model of 3-month real bone ingrowth, the regenerated tissues growing on the scaffold have already attached to the surrounding tissues and formed a part. According the previous in-vivo tests [23], it is found that the scaffold has a good connection with bone tissues. In that case, it is assumed that the contact type between the bone and the scaffold is bonding. In the model with 100% bone ingrowth, all the void space in the scaffold is fulfilled with regenerated bone tissues, which is an ideal circumstance for tissue engineering. The connection type between the scaffold and the bone setting is set as bonded with no doubt. Because different sheep knees are different in curvature, area, geometry, and weight, different pressure loadings are applied, which are 2.5, 5, 7.5, 10, 12.5 and 15 MPa. Mesh convergence analyses are carried out, and 3 physical with an initial 0% bone ingrowth, a 3-month percentage of bone ingrowth, and 100% bone ingrowth have 905082, 4289685 and 3404138 elements respectively with hexahedra and tetrahedra 2 types of elements shown in Fig. 6.

3 Results

In most of the scaffold designs, cylinder structure and cubic structure are most commonly used. According to the previous in-vivo tests using a bionic 3D scaffold with truncated cone geometry, the scaffold would sink 2 or 3 mm deeper to the trabecular bone compared to its original position shown in Fig. 7. In that case, to find out the main reason causing this problem is important.

There are two main reasons that cause the scaffold to loosen the fixation with surrounding tissues and subsidence, which are dynamic loading and bone reabsorption. As bone reabsorption is related to scaffold material properties, FE is used to investigate how the scaffold structures influence the subsidence problem. According to the previous in-vivo tests, a special tapered (truncated cone) instead of the cylinder structure is used to manufacture the scaffold. Compared to the cylinder, the truncated cone can provide more contact surfaces with surrounding tissues, and get vertical support force and friction force from surrounding tissues to help it fix with those tissues, but the cylinder structure scaffold can only get friction force from the surrounding tissues, which can be seen in Fig. 8.

With nearly the same macro parameters of the scaffold geometry, it can be easily predicted that the truncated cone structure will provide a better bioperformance than the normal design. As for truncated cone structure FEA, the deformation and the maximum Von-Mises stress of the bottom face are shown in Fig. 9 by different applied loadings .

In general, the sheep knee joint can endure 5-10 Mpa pressure during normal activity. With up to 15 Mpa applied loading, the results show that the maximum deformation is below 0.09mm. In the pressure range of 5-10 Mpa, the deformation is around 0.02-0.04 mm. The maximum deformation is shown in the scaffold with real bone ingrowth (3 month), which can reach nearly 0.065 mm. It is shown that the scaffold at the initial stage does not show much worse deformation than that with regenerated bone in the inner structure and connected with surrounding tissues. Compared to in-vivo tests, the difference of deformation between the scaffold at the initial stage and that after 3 months' healing process is far greater than the difference in deformation caused by the loading. It seems the bone reabsorption process, in which osteoclasts break the bone tissue down and transfer the calcium from bone tissue to blood [31], plays a more important role in scaffold subsidence than loading. There is no doubt that the cyclic loading and frictional stress would cause bone reabsorption. Further experimental and simulation tests are needed to investigate how the loading influence bone reabsorption using additive manufacturing designed 3D porous scaffold. Moreover, the bone loss is also caused by stress shielding, as the metallic implant-Young's modulus is far higher than surrounding tissues, which means that a scaffold with higher porosity and higher strength is needed [32].

With more new bone tissues growing on the scaffold surface and connected with the surrounding tissues, the titanium scaffold will suffer less loading pressure, as shown in Fig. 10 to the left.

4 Discussion

To match the requirement of pore size, porosity, and surface area, scaffold often faced a subsidence problem during healing process. The reason is complex and it is hard to define which one is the main factor. It is essential to ensure the mechanical fixation of the scaffold when it put into the target area.

Evaluating the mechanical fixation of the scaffold at the initial stage is challenging because no facility can be put into the target area. Further, to sacrifice animals at initial stage or 1 month is too expensive because *in vivo* studies for tissue engineering products need to be at least 3 months. Aiming to create suitable numerical models for bone-scaffold interaction, 3 months sheep study has been done. From 3 months results, the percentage of bone regeneration in each pore of the scaffold is analyzed by MATLAB program according to the 2D Micro-CT scanned images. To analysis the interaction, the physical model is created based on the regenerated bone ingrowth percentage of *in vivo* tests.

To investigate the scaffold would endure or fail during the healing process, von-Mises stress is calculated. As the stress on the scaffold during the healing process is not at a constant value, considering bone ingrowth while evaluating the fatigue performance of the scaffold is important [33], and it should be well investigated in the future. According to Fig. 10 to the right, the surrounding tissues suffer less when more regenerated bone grew on the scaffold inside. In the real bone model, it is assumed that regenerated bone connected well with the surrounding tissues, which cannot be observed or tested, so the real stress that surrounding tissues would suffer in the real bone model (3-months model) would be much higher than the simulation results.

To obtain the optimal scaffold macro design, the evaluation of the effect of each specific scaffold parameter on tissue regeneration needs huge costs and long-term experiments. The realistic physical model (scaffold with regenerated tissues) after 3 months' in-vivo tests is constructed. According to in-vivo tests, the scaffold could not maintain its original position and would subsidence 1-2 mm in the target area compared to its original position, but the simulation results showed that the scaffold could only sink less than 0.1 mm. In that case, to evaluate this situation more properly, further experimental studies are needed to find the relationship between scaffold material, structure, loading magnitude and bone reabsorption.

5 Conclusion

For obtaining the optimal scaffold macro design, the evaluation of the effect of each specific scaffold parameter on tissue regeneration needs huge cost and long-term research. In this study, the in vivo tests for realistic physical model (scaffold with regenerated tissue) were constructed. The scaffold could not maintain its original position and sink 1-2 mm in the target area. However, the FEA showed that the subsidence of scaffold is less than 0.1mm. The result of this study suggested that mechanical loading is not the main reason for scaffold subsidence. Further experimental studies are needed to find the relationship between scaffold material, structure, loading magnitude and bone loss (bone reabsorption).

Acknowledgments

This work was supported by Versus Arthritis Research UK (Grant No: 21977), European Commission via a H2020-MSCA-RISE programme (BAMOS, Grant No: 734156), Innovative UK via

Newton Fund (Grant No:102872), Engineering and Physical Science Research Council (EPSRC) via DTP CASE programme (Grant No: EP/T517793/1), and Intergovernmental cooperation in science and technology of China (No. 2016YFE0125300).

Declarations

Ethical Statement

All animals were kept in a pathogen-free environment and fed ad lib. The procedures for care and use of animals were approved by the Animals (Scientific Procedures) Act (ASPA). All applicable institutional and governmental regulations concerning the ethical use of animals were followed.

Conflicts of interest

The authors declare that they have no conflict of interests.

References

[1] Hollister SJ. Porous scaffold design for tissue engineering. Nat Mater. 2005;4:518-90.
[2] Rice MA, Dodson BT, Arthur JA, and Anseth KS. Cell-based therapies and tissue engineering. Otolaryngol Clin North Am. 2005;38:199-214. https://doi.org/10.1016/j.otc.2004.10.010.
[3] Langer R and Vacanti JP. Tissue Engineering. Science. 1993;260:920-6.
[4] Hubbell JA. Bioactive biomaterials. Biochem Eng J. 1999;10:123-9.
[5] Healy KE. Molecular engineering of materials for bioreactivity. Curr Opin Solid State Mater Sci. 1999;4:381-7.
[6] Karageorgiou V and Kaplan D. Porosity of 3D biomaterial scaffolds and osteogenesis. Biomaterials. 2005;26:5474-91. https://doi.org/10.1016/j.biomaterials.2005.02.002.
[7] Burr DB and Gallant MA. Bone remodelling in osteoarthritis. Nat Rev Rheumatol. 2012;8:665-73. https://doi.org/10.1038/nrrheum.2012.130.
[8] Wu S, Liu X, Yeung KWK, Liu C, and Yang X. Biomimetic porous scaffolds for bone tissue engineering. Mater Sci Eng R Rep. 2014;80:1-36. https://doi.org/10.1016/j.mser.2014.04.001.
[9] Hutmacher DW. Scaffolds in tissue engineering bone and cartilage. Biomaterials. 2000;21:2529-43.
[10] Uematsu K, Hattori K, Ishimoto K, Yamauchi J, Habata T, Takakura Y, Ohgushi H, Fukuchi T, Sato M. Cartilage regeneration using mesenchymal stem cells and a three-dimensional poly-lactic-glycolic acid (PLGA) scaffold. Biomaterials. 2005;26:4273-9. https://doi.org/10.1016/j.biomaterials.2004.10.037.
[11] Balakrishnan B, Joshi N, Jayakrishnan A, and Banerjee R. Self-crosslinked oxidized alginate/gelatin hydrogel as injectable, adhesive biomimetic scaffolds for cartilage regeneration. Acta Biomater. 2014;10:3650-63. https://doi.org/10.1016/j.actbio.2014.04.031.
[12] Tamai N, Myoui A, Hirao M, Kaito T, Ochi T, Tanaka J, Takaoka K, Yoshikawa H. A new biotechnology for articular cartilage repair: subchondral implantation of a composite of interconnected porous hydroxyapatite, synthetic polymer (PLA-PEG), and bone morphogenetic protein-2 (rhBMP-2). Osteoarthr Cartil. 2005;13:405-17. https://doi.org/10.1016/j.joca.2004.12.014.

[13] Rosenzweig DH, Carelli E, Steffen T, Jarzem P, and Haglund L. 3D-Printed ABS and PLA Scaffolds for Cartilage and Nucleus Pulposus Tissue Regeneration. Int J Mol Sci. 2015;16:15118-35. https://doi.org/10.3390/ijms160715118.

[14] Yavari SA, Wauthle R, van der Stok J, Riemslag AC, Janssen M, Mulier M, Kruth JP, Schrooten J, Weinans H, Zadpoor AA. Fatigue behavior of porous biomaterials manufactured using selective laser melting. Mater Sci Eng C Mater Biol Appl. 2013;33:4849-58. https://doi.org/10.1016/j.msec.2013.08.006.

[15] Spoerke ED, Murray NG, Li H, Brinson LC, Dunand DC, and Stupp SI. A bioactive titanium foam scaffold for bone repair. Acta Biomater. 2005;1:523-33. https://doi.org/10.1016/j.actbio.2005.04.005.

[16] Hofmann AA, Bloebaum RD, and Bachus KN. Progression of human bone ingrowth into porous-coated implants:Rate of bone ingrowth in humans. Acta Orthop Scand. 1997;68:161-6. https://doi.org/10.3109/17453679709004000.

[17] Schliephake H, Neukam EW, and Klosa D. Influence of pore dimensions on bone ingrowth into porous hydroxylapatite blocks used as bone graft substitutes.A histometric study. Int J Oral Maxillofac Surg. 1991;20:53-8.

[18] Hulbert SF, Young FA, Mathews RS, Klawitter JJ, Talbert CD, and Stelling FH. Potential of Ceramic Materials as Permanently Implantable Skeletal Prostheses. J Biomed Mater Res. 1970;4:433-56.

[19] Knecht S, Erggelet C, Endres M, Sittinger M, Kaps C, and Stussi E. Mechanical testing of fixation techniques for scaffold-based tissue-engineered grafts. J Biomed Mater Res B Appl Biomater. 2007;83:50-7. https://doi.org/10.1002/jbm.b.30765.

[20] Peterson L, Minas T, Brittberg M, Nilsson A, Sjogren-Jansson E, and Lindahl A. Two- to 9-Year Outcome After Autologous Chondrocyte Transplantation of the Knee. Clin Orthop Relat Res. 2000;374:212-34.

[21] Nehrer S, Spector M, and Minas T. Histologic analysis of tissue after failed cartilage repair procedures. Clin Orthop Relat Res. 1999;365:149-62.

[22] Dabrowski B, Swieszkowski W, Godlinski D, and Kurzydlowski KJ. Highly porous titanium scaffolds for orthopaedic applications. J Biomed Mater Res B Appl Biomater. 2010;95:53-61. https://doi.org/10.1002/jbm.b.31682.

[23] Liu Z, Tamaddon M, Gu Y, Yu J, Xu N, Gang F, Sun X, Liu C. Cell Seeding Process Experiment and Simulation on Three-Dimensional Polyhedron and Cross-Link Design Scaffolds. Biotechnol Bioeng. 2020;8:104. https://doi.org/10.3389/fbioe.2020.00104.

[24] Keaveny TM. Biomechanics of Trabecular Bone. Annu Rev Biomed Eng. 2001;3:307-33.

[25] Fermor HL, McLure SW, Taylor SD, Russell SL, Williams S, Fisher J, Ingham E. Biological, biochemical and biomechanical characterisation of articular cartilage from the porcine, bovine and ovine hip and knee. Biomed Mater Eng. 2015;25:381-95. https://doi.org/10.3233/BME-151533.

[26] Wu ZX, Lei W, Hu YY, Wang HQ, Wan SY, Ma ZS, Sang HX, Fu SC, Han YS. Effect of ovariectomy on BMD, micro-architecture and biomechanics of cortical and cancellous bones in a sheep model. Med Eng Phys. 2008;30:1112-8. https://doi.org/10.1016/j.medengphy.2008.01.007.

[27] Mittra E, Rubin C, and Qin YX. Interrelationship of trabecular mechanical and microstructural properties in sheep trabecular bone. J Biomech. 2005;38:1229-37. https://doi.org/10.1016/j.jbiomech.2004.06.007.

[28] Andrish J and Holmes R. Effects of Synovial Fluid on Fibroblasts in Tissue Culture. Clin Orthop Relat Res. 1979:279-83.

[29] Hazelton RA, Vedam R, Masci PP, and Whitaker AN. Partial purification and characterisation of a synovial fluid inhibitor of osteoblasts. Ann Rheum Dis. 1990;49:121-4.

[30] Popov VL. Contact Mechanics and Friction:Physical Principles and Applications: Springer Heidelberg Dordrecht London New York, 2011.

[31] Teitelbaum SL. Bone Reabsorption by Osteoclasts. Bone remodeling and repair. 2000;289:1504-8.

[32] Cheong VS, Fromme P, Mumith A, Coathup MJ, and Blunn GW. Novel adaptive finite element algorithms to predict bone ingrowth in additive manufactured porous implants. J Mech Behav Biomed Mater. 2018;87:230-239. https://doi.org/10.1016/j.jmbbm.2018.07.019

[33] Cheong VS, Fromme P, Coathup MJ, Mumith A, and Blunn GW. Partial Bone Formation in Additive Manufactured Porous Implants Reduces Predicted Stress and Danger of Fatigue Failure. Ann Biomed Eng. 2020;48:502-514. https://doi.org/10.1007/s10439-019-02369-z.

Figures

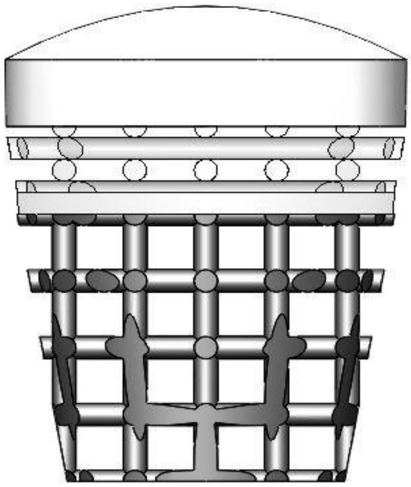

Fig. 1 Bone Structure and bionic osteochondral scaffold

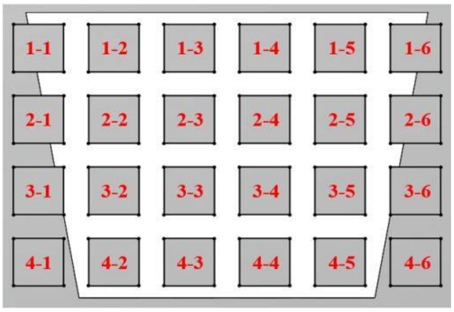

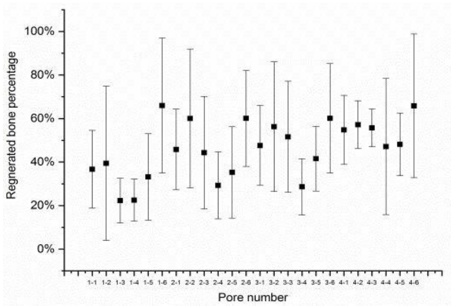

Fig. 2 Bionic osteochondral scaffold pore number; Regenerated bone percentage in each pore

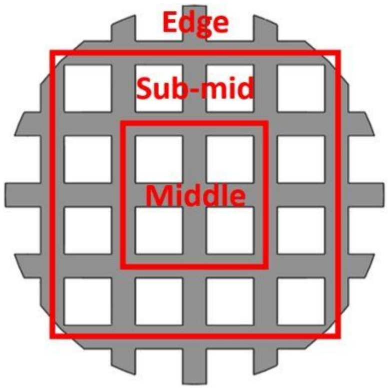

Fig. 3 Regions of osteochondral scaffold: edge, sub-mid and middle

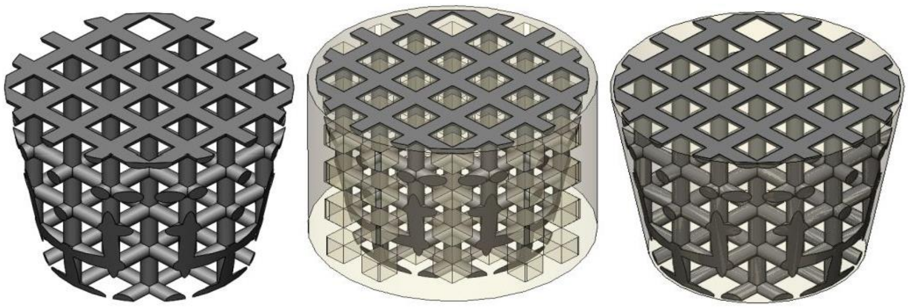

Fig. 4 a.0% bone ingrowth at the beginning; b.3-month real bone ingrowth; c.100% bone ingrowth

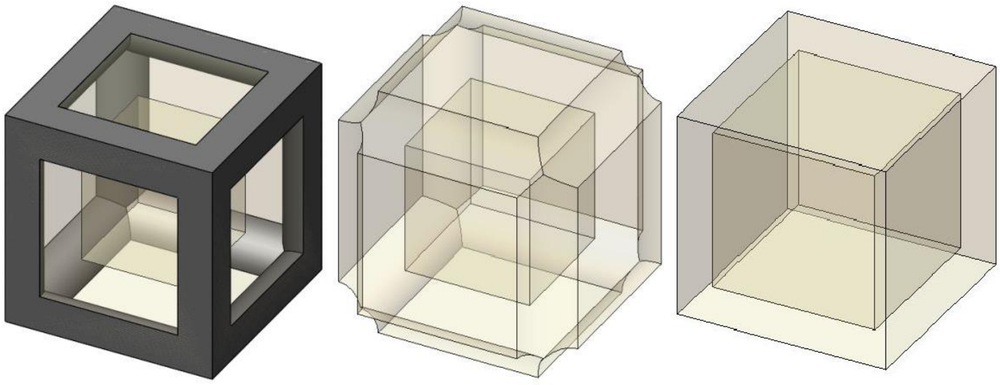

Fig. 5 a. 3-month real bone ingrowth unit cell; b. 3-month real bone ingrowth unit cell assumption; c. 3-month real bone ingrowth unit cell for FE analysis

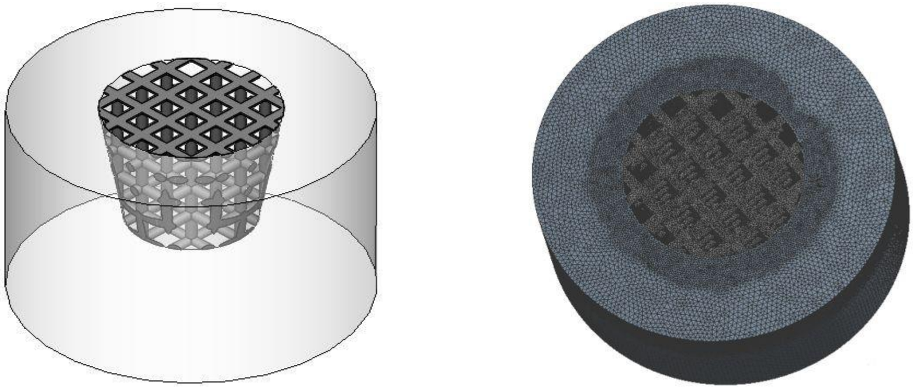

Fig. 6 FE model and mesh of the 0% bone ingrowth

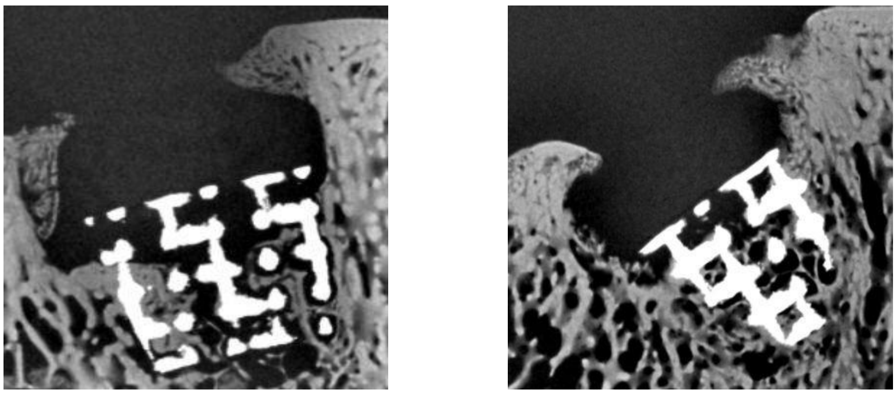

Fig. 7 X-ray of slices of trabecular bone and scaffold

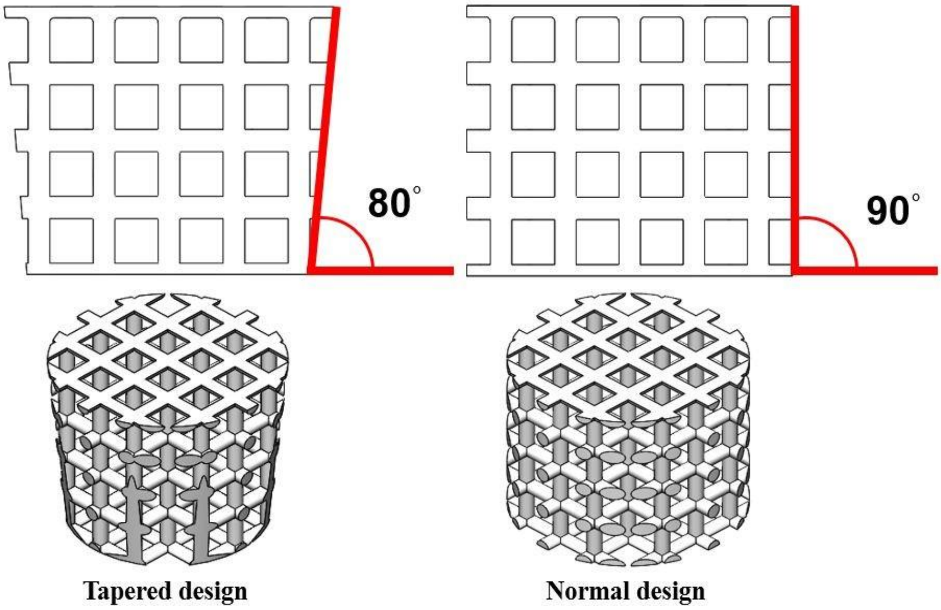

Fig. 8 Tapered design (truncated cone) and normal design (cylinder)

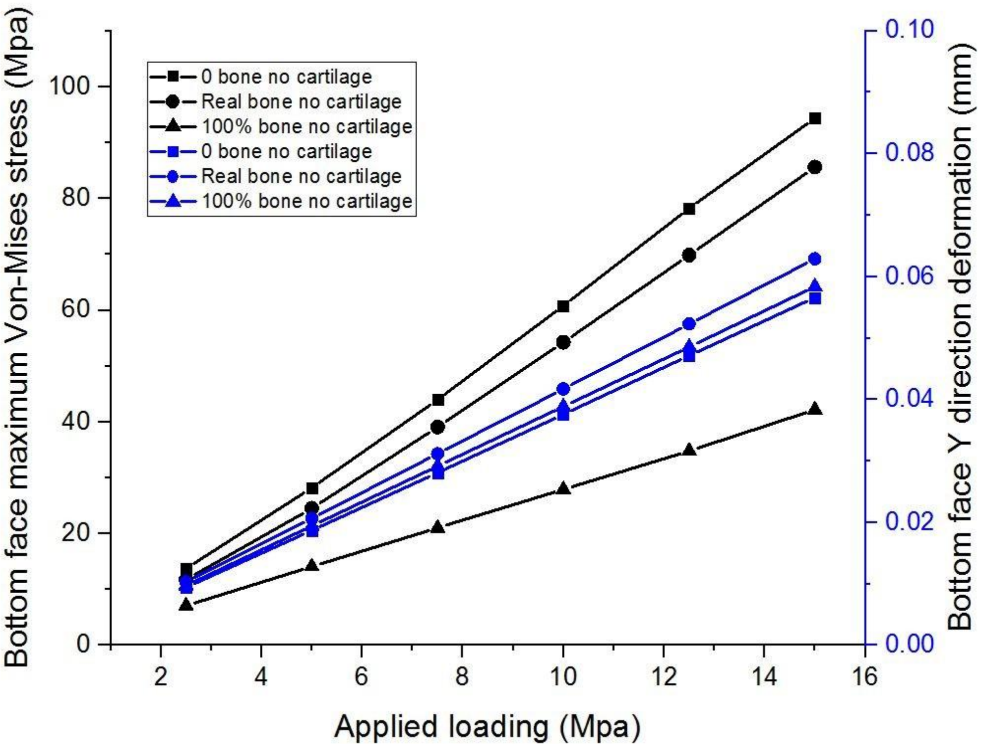

Fig. 9 Deformation and maximum Von-Mises stress of the bottom face by different applied loadings

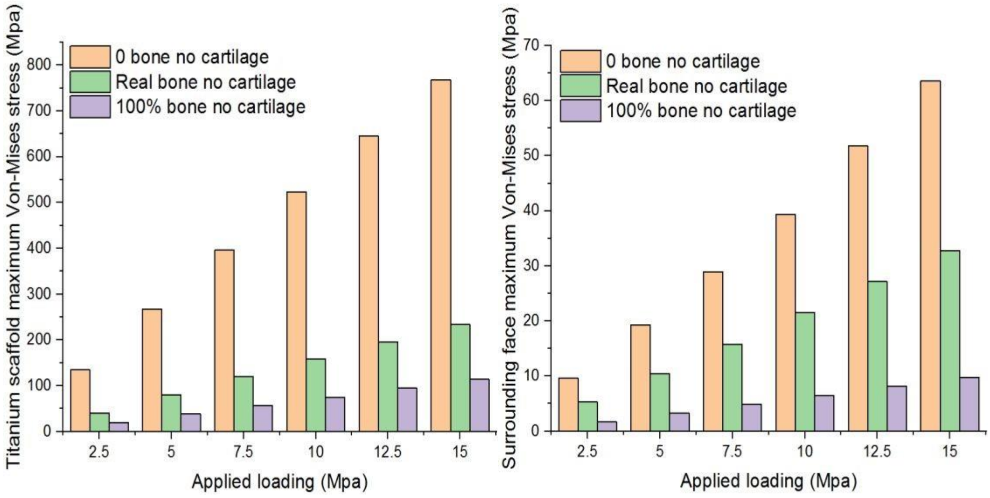

Fig. 10 Maximum Von-Mises stress of the titanium scaffold by different applied loadings (left);

Maximum Von-Mises stress of the surrounding tissue by different applied loadings (right)